Conformal Prediction for Compositional Data

Lucas P. Amaral^{1, 2}, Luben M. C. Cabezas^{1,2}, Thiago R. Ramos¹, and Gustavo H. A. Pereira¹

¹Department of Statistics, Federal University of São Carlos ²Institute of Mathematics and Computer Science, University of São Paulo

In this work, we propose a set of conformal prediction procedures tailored to compositional responses, where outcomes are proportions that must be positive and sum to one. Building on Dirichlet regression, we introduce a split conformal approach based on quantile residuals and a highest-density region strategy that combines a fast coordinate-floor approximation with an internal grid refinement to restore sharpness. Both constructions are model-agnostic at the conformal layer and guarantee finite-sample marginal coverage under exchangeability, while respecting the geometry of the simplex. A comprehensive Monte Carlo study spanning homoscedastic and heteroscedastic designs shows that the quantile residual and grid-refined HDR methods achieve empirical coverage close to the nominal 90% level and produce substantially narrower regions than the coordinate-floor approximation, which tends to be conservative. We further demonstrate the methods on household budget shares from the BudgetItaly dataset, using standardized socioeconomic and price covariates with a train, calibration, and test split. In this application, the grid-refined HDR attains coverage closest to the target with the smallest average widths, closely followed by the quantile residual approach, while the simple triangular HDR yields wider, less informative sets. Overall, the results indicate that conformal prediction on the simplex can be both calibrated and efficient, providing practical uncertainty quantification for compositional prediction tasks.

Keywords: Compositional data, Conformal prediction, Dirichlet regression, High density, Non-conformity measure

1. Introduction

Compositional data (CoDa) are widely used across many fields whenever the goal is to model the parts of a whole. Typical examples include ecology, to quantify species shares in an ecosystem (Greenacre, 2021), medicine, to measure the concentrations of different cell types in a patient's blood (Zhang *et al.*, 2025), among others. A compositional observation is a vector $\mathbf{y} = (y_1, \ldots, y_D)^{\mathsf{T}}$ of positive components such that $\sum_{j=1}^{D} y_j = 1$. The set

$$\Delta_D = \{(y_1, \dots, y_D) \in \mathbb{R}^D : \sum_{j=1}^D y_j = 1, \ y_j > 0, \ j = 1, \dots, D\}$$

is denoted the (D-1)-simplex. CoDa can be analyzed in several ways, but modeling is more used due to the simplex constraints. Over the years, however, substantial progress has been made (see Alenazi (2023)). The simplex is the natural sample space for these data (Aitchison, 1982), and the Dirichlet family is a common probabilistic model on this space (Barndorff-Nielsen & Jørgensen, 1991). In regression contexts, Dirichlet regression models (Hijazi & Jernigan, 2009) are frequently employed and can be viewed as generalizations of beta regression models (Ferrari & Cribari-Neto, 2004). Parametric modeling often emphasizes the interpretability of regression coefficients and the verification of modeling assumptions, as these directly affect the goodness of fit.

Nevertheless, in many practical scenarios, the primary focus lies in the prediction of new observations and their respective predictive intervals. When response variables are constrained to the unit interval (0,1) — as is the case for proportions or fractions —, traditional approaches based on normality assumptions are often inadequate. In these cases, there are established methodologies that rely on resampling techniques (bootstrap) and employ the residuals as surrogates to estimate the prediction error (Espinheira et al., 2014; Cribari-Neto & Lima, 2021). However, such methods typically rely on asymptotic theory and may require large samples to achieve accurate coverage. Moreover, standard bootstrap procedures may be ill–suited under heteroscedasticity, as this can undermine exchangeability and lead to invalid inference and predictions. Recently, Wu et al. (2025) proposed conformalized methods for bounded outcomes within the broader Conformal Prediction (CP) framework (Vovk et al., 2005; Shafer & Vovk, 2008; Papadopoulos et al., 2008; Lei et al., 2018), offering a machine-learning-based approach to construct prediction intervals with finite—sample guarantees, including marginal and asymptotic conditional validity.

Inspired by this successful adaptation to bounded data, we leverage the fundamental principles of CP(Vovk et al., 2005; Shafer & Vovk, 2008; Lei et al., 2018). CP is a distribution–free and model–agnostic framework highly valued for providing marginal coverage guarantees in finite samples under the mild assumption of exchangeability. This assumption is often reasonable in various data settings and allows CP to be coupled with a wide range of statistical models and learning algorithms (Angelopoulos & Bates, 2021). The core ingredient of this framework is the nonconformity score, a function that quantifies how atypical a data point is relative to a model trained on the remaining data.

Numerous extensions for general regression models have been studied (Tibshirani et al., 2019), along with proposals for constructing nonconformity scores in different contexts (Kato et al., 2023). A persistent challenge in modeling is heteroscedasticity, i.e., when the response variance varies with covariates. In Dirichlet regression, the mean and variance are intrinsically linked; thus, dispersion is naturally accommodated by the model. To address heteroscedasticity within conformal prediction, several adaptations have been developed, including conformalized quantile regression (Romano et al., 2019), normalized conformal prediction (Papadopoulos et al., 2008; Lei et al., 2018; Kato et al., 2023), and Mondrian conformal prediction (Boström & Johansson, 2020; Cabezas et al., 2025; Dewolf et al., 2025).

A model-based extension of conformal prediction tailored to distributional regression was introduced by Chernozhukov *et al.* (2021). Their approach uses the probability integral transform (PIT) to define nonconformity measures from an estimated conditional distribution of the response, yielding asymptotically valid prediction intervals under heteroscedasticity. Some related works, Tibshirani *et al.* (2019); Barber *et al.* (2023) propose conformal prediction algorithms based

on weighted quantiles that deliver finite-sample guarantees in broad, non-exchangeable scenarios.

Inspired by these ideas, this work proposes conformal prediction methods for compositional data. The paper is organized as follows. Section 2 presents two parameterizations of the Dirichlet distribution and the corresponding regression specification. Section 3 details our approach for constructing conformal prediction sets for Dirichlet regression using (i) randomized quantile residuals (Dunn & Smyth, 1996) of the marginal components, (ii) an approximation to the highest density region (HDR) that contains the exact prediction set, and (iii) a grid search within the resulting polytope to mitigate overcoverage and overly wide intervals. Section 4 describes the simulation design and reports results for the three predictive methods, evaluating empirical coverage, interval widths, and runtime. Section 5 presents a real-data application. Section 6 concludes with a general discussion and avenues for future work. R code and data can be found in the GitHub repository https://github.com/LucAmaralDS/CP-dirichlet.

2. Regression models for compositional data

Consider a regression setting involving CoDa, where the *D*-part response vector $\mathbf{Y}_i = (Y_{i1}, \dots, Y_{iD})^{\top}$ for the *i*-th observation, $i = 1, \dots, n$, belongs to the D-dimensional simplex, $\mathbf{Y}_i \in \Delta_D$. In many CoDa regression problems, we assume that the response \mathbf{Y}_i follows a Dirichlet distribution with shape parameters $\boldsymbol{\lambda}_i = (\lambda_{i1}, \dots, \lambda_{iD})^{\top}$, where $\lambda_{ij} > 0$ for all $j = 1, \dots, D$. The probability density function (PDF) for a general compositional vector \mathbf{Y} following Dirichlet($\boldsymbol{\lambda}$) is given by:

$$f(\mathbf{y}; \boldsymbol{\lambda}) = \frac{\Gamma(\sum_{j=1}^{D} \lambda_j)}{\prod_{j=1}^{D} \Gamma(\lambda_j)} \prod_{j=1}^{D} y_j^{\lambda_j - 1}, \quad \mathbf{y} \in \Delta_D$$

where $\Gamma(\cdot)$ is the Gamma function.

Let $\lambda_0 = \sum_{t=1}^D \lambda_t$. For the Dirichlet distribution, the mean and variance are, respectively,

$$\mathbb{E}[Y_j] = \frac{\lambda_j}{\lambda_0}$$
 and $\operatorname{Var}(Y_j) = \frac{\lambda_j(\lambda_0 - \lambda_j)}{\lambda_0^2(\lambda_0 + 1)}$.

For regression problems, where the response \mathbf{Y}_i is linked to a vector of covariates \mathbf{X}_i , it is common to adopt a Dirichlet parameterization that models the mean of the response components (μ_j) together with a precision parameter (ϕ) , yielding more direct interpretability of the estimated coefficients. We define the reparameterization by letting $\phi = \sum_{j=1}^{D} \lambda_j$ and $\mu_j = \lambda_j/\phi$, for $j = 1, \ldots, D$, with $\sum_{j=1}^{D} \mu_j = 1$. The density function under this alternative mean-precision parameterization is given by:

$$f(\mathbf{y}; \mu_1, \dots, \mu_D, \phi) = \frac{\Gamma(\phi)}{\prod_{j=1}^D \Gamma(\mu_j \phi)} \prod_{j=1}^D y_j^{\phi \mu_j - 1}$$
(1)

where $0 < \mu_j < 1$ for all j and $\phi > 0$. Under this setup, the expected value and variance of the j-th component are, respectively:

$$\mathbb{E}[Y_j] = \mu_j \quad \text{and} \quad \operatorname{Var}[Y_j] \ = \ \frac{\mu_j(1 - \mu_j)}{\phi + 1} = \frac{V(\mu_j)}{\phi + 1}.$$

The term ϕ is thus a precision parameter, as larger values lead to smaller variance.

Let Y_1, \ldots, Y_n and $\mathbf{Y}_i = (Y_{i1}, \ldots, Y_{iD})^{\top}$ be random variables distributed according to a Dirichlet distribution as in Eq. (1). The systematic components of the logistic Dirichlet regression model are given by

$$\log\left(\frac{\mu_{ij}}{\mu_{i1}}\right) = x_{ij1}\beta_{j1} + x_{ij2}\beta_{j2} + \dots + x_{ijp_j}\beta_{jp_j}, \quad 2 \le j \le D,$$

$$\log(\phi_i) = d_{i1}\gamma_1 + d_{i2}\gamma_2 + \dots + d_{ip_n}\gamma_{p_n},$$
(2)

 $(x_{ij1}, x_{ij2}, \ldots, x_{ijp_j}, d_{i1}, d_{i2}, \ldots, d_{ip_{\phi}})^{\top}$ are the covariates and $(\beta_{j1}, \beta_{j2}, \ldots, \beta_{jp_j}, \gamma_1, \gamma_2, \ldots, \gamma_{p_{\phi}})^{\top}$ unknown parameters. We adopt a logit link for the mean vector and a logarithmic link for the precision parameter, in line with the conventional parametrization of multinomial logistic regression (Hosmer Jr et al., 2013). This specification is particularly convenient because it yields regression coefficients with a transparent interpretation and automatically restricts the precision parameter to the positive real line, satisfying the distributional constraint $\phi > 0$. The parameters of model (2) are estimated by maximum likelihood, and all empirical results reported here are obtained using the DirichletReq package (Maier, 2014) in R.

3. Conformal prediction for compositional data regression models

A common practice in regression analysis is to use a fitted model to predict out-of-sample or missing response values. While a point prediction can be readily obtained from the fitted model, it is often desirable to accompany it with a prediction region at a prescribed coverage level. In this section, we present our proposals for constructing conformal prediction regions in Dirichlet regression models. Section 3.1 introduces the conformal prediction framework and the specific algorithm used throughout, namely split conformal prediction. In Section 3.2, we construct prediction regions using quantile residuals (Dunn & Smyth, 1996) as nonconformity scores. Section 3.3 instead uses the negative log-likelihood as the nonconformity score and inverts it to obtain a highest-density prediction region, which we approximate by coordinate-floor. The associated convex optimization formulation underlying this approximation is presented in Section 3.4.

3.1. Conformal prediction

Recently, conformal prediction (CP) methods have been widely employed for constructing prediction regions under weak assumptions (Vovk et al., 2005; Shafer & Vovk, 2008). Given an exchangeable sample of pairs (X_i, Y_i) , i = 1, ..., n, conformal prediction is used to produce a prediction set $C(\cdot)$ for a new covariate vector X_{n+1} with unknown response Y_{n+1} , in such a way that $\mathbb{P}(Y_{n+1} \in C(X_{n+1})) \geq 1 - \alpha$.

The literature offers several algorithms for constructing such prediction sets, including Full Conformal Prediction (FCP) (Vovk et al., 2005), Split Conformal Prediction (SCP) (Papadopoulos et al., 2008; Vovk, 2012; Lei et al., 2018), and Jackknife+ (Barber et al., 2021). Given the computational burden of FCP, especially with multivariate responses, we adopt the Split Conformal Prediction (SCP) method. SCP partitions the available data into a training set ($\mathcal{D}_{\text{train}}$) and a calibration set (\mathcal{D}_{cal}). While the model is fitted only on $\mathcal{D}_{\text{train}}$, this data splitting incurs a trade-off in statistical power, potentially leading to wider prediction sets.

The core ingredient of CP is the nonconformity score, denoted by $s(\mathbf{X}, \mathbf{Y})$, which is defined as a function $s: \mathcal{X} \times \mathcal{Y} \to \mathbb{R}$ that quantifies how atypical a new observation (\mathbf{X}, \mathbf{Y}) is relative to the model trained on the remaining data. For a given significance level $\alpha \in (0, 1)$, the resulting $(1-\alpha)$ -level SCP prediction region, $\mathcal{C}_{1-\alpha}(\mathbf{X}^*)$, is generally defined over the response domain \mathcal{Y} as:

$$C_{1-\alpha}(\mathbf{X}^*) = \{ \mathbf{y}^* \in \mathcal{Y} : s(\mathbf{X}^*, \mathbf{y}^*) \le \hat{q}_{1-\alpha} \}$$

where $\hat{q}_{1-\alpha}$ is the empirical quantile of order $\lceil (1-\alpha)(n_{\rm cal}+1) \rceil$ of the nonconformity scores calculated on the calibration set $\mathcal{D}_{\rm cal}$. This region provides a marginal coverage guarantee of at least $1-\alpha$ in finite samples under the assumption of exchangeability.

In CP approaches, the choice of $s(\mathbf{x}, \mathbf{y})$ is critical, as it directly influences the shape and informativeness of the resulting predictive regions (Angelopoulos & Bates, 2021; Izbicki, 2025). In standard Euclidean regression, a common choice for $s(\mathbf{x}, y)$ is the absolute residual, $|y - \widehat{\mathbb{E}}[Y|\mathbf{x}]|$

(Lei et al., 2018), where $\widehat{\mathbb{E}}[Y|\mathbf{x}]$ is the estimated regression function fitted on the training data.

However, the compositional nature of our data (constrained to the simplex Δ_D) and the use of the Dirichlet distribution necessitate scores that naturally account for the distribution's properties and the intrinsic geometry. For this reason, we focus on constructing prediction regions over the simplex Δ_D . We specifically opt to use nonconformity scores based on the quantile residual (Dunn & Smyth, 1996) and the negative log-likelihood, which are detailed in the following sections. The full procedure for constructing the prediction regions using these specific scores is detailed in Algorithms 1 and 2, which appear in Appendix B.

3.2. Predictive sets with quantile residuals

For Dirichlet regression, we propose a split conformal approach based on quantile residuals. The marginal distributions under a Dirichlet law are beta (Lin, 2016), we have $Y_j \sim \text{Beta}(\lambda_j, \sum_{t=1}^D \lambda_t - \lambda_j)$. Let a Dirichlet regression model be fitted as in Eq. (2), returning the estimated parameters $\hat{\lambda}(\mathbf{x}) = (\hat{\lambda}_1, \dots, \hat{\lambda}_D)$ and $\hat{\lambda}_0(\mathbf{x}) = \sum_{d=1}^D \hat{\lambda}_d(\mathbf{x})$. It follows that, conditionally on covariates $\mathbf{X} = \mathbf{x}$,

$$Y_j \mid \mathbf{X} = \mathbf{x} \sim \text{Beta}(\widehat{\lambda}_j(\mathbf{x}), \ \widehat{\lambda}_0(\mathbf{x}) - \widehat{\lambda}_j(\mathbf{x})).$$
 (3)

Leveraging this property, we define the conformity score via quantile residuals. By definition, the (randomized) quantile residual of Dunn & Smyth (1996) is

$$r_{ij}^{q} = \Phi^{-1}\left\{F(y_{ij}; \widehat{\mu}_{ij}, \widehat{\phi}_{ij})\right\}, \tag{4}$$

where $\Phi(\cdot)$ and $F(\cdot)$ denote the cumulative distribution functions (CDFs) of the standard normal distribution and of the marginal beta distribution for component j, respectively. To obtain a joint prediction region that controls all components simultaneously, one might consider multivariate scores (e.g., Mahalanobis ellipses; Ghorbani, 2019). However, such choices hinder analytic inversion and typically require grid search to recover marginal intervals. In light of this, we adopt the following max-type conformity score:

$$S(\mathbf{x}, \mathbf{y}) = \max_{j} |Z_{j}(\mathbf{x}, \mathbf{y})|, \tag{5}$$

where $Z_j = \Phi^{-1}(U_j)$, $U_j = F_{\text{Beta}_j}(y_{ij})$, and $\text{Beta}_j = \text{Beta}(\widehat{\lambda}_j(\mathbf{x}), \widehat{\lambda}_0(\mathbf{x}) - \widehat{\lambda}_j(\mathbf{x}))$. By definition, the predictive set is

$$C_{\text{split}}(\mathbf{x}) = \{ \mathbf{y} \in \Delta_D : S(\mathbf{x}, \mathbf{y}) \le q_{1-\alpha} \}.$$

The condition $S(\mathbf{x}, \mathbf{y}) \leq q_{\alpha}$ is equivalent, componentwise, to

$$-q_{1-\alpha} \le Z_j(\mathbf{x}, \mathbf{y}) \le q_{1-\alpha} \iff \Phi(-q_{1-\alpha}) \le U_j(\mathbf{x}, \mathbf{y}) \le \Phi(q_{1-\alpha}),$$

since the normal CDF $\Phi(\cdot)$ is monotone and $Z_j = \Phi^{-1}(U_j)$. Hence, defining $p_{\inf} = \Phi(-q_\alpha)$ and $p_{\sup} = \Phi(q_\alpha)$, we obtain the closed marginal intervals on the original response scale,

$$I_j = \left[F_{\operatorname{Beta}_j}^{-1}(p_{\operatorname{inf}}), F_{\operatorname{Beta}_j}^{-1}(p_{\operatorname{sup}}) \right],$$

and therefore

$$C_{\text{split}}(\mathbf{x}) = \{ \mathbf{y} \in \Delta_D : y_i \in I_i(\mathbf{x}) \ \forall i \}.$$

This method, however, does not naturally yield marginal intervals that adhere to the constraint $\sum_j y_j = 1$. This is because the prediction intervals are generated marginally for each component. Consequently, in the following section, we propose a method based on a floor approximation for the prediction region that respects the simplex constraint.

3.3. Density-based conformal sets on the simplex: HDR with coordinate-floor approximation

Consider (x_i, y_i) with $y_i \in \Delta_D := \{ \mathbf{y} \in \mathbb{R}^D : \sum_{j=1}^D y_j = 1 \}$. Suppose that, given x, the model provides parameters

$$\lambda(\mathbf{x}) = (\lambda_1(\mathbf{x}), \dots, \lambda_D(\mathbf{x})), \qquad \lambda_j(\mathbf{x}) = \phi(\mathbf{x}) \,\mu_j(\mathbf{x}), \quad \sum_{j=1}^D \mu_j(\mathbf{x}) = 1, \quad \phi(\mathbf{x}) > 0.$$

Under a Dirichlet distribution with density given in (1), the nonconformity score is

$$s(\mathbf{x}, \mathbf{y}) = -\log f(\mathbf{y} \mid \mathbf{x}) = -\log \Gamma(\phi) + \sum_{j=1}^{D} \log \Gamma(\mu_j \phi) - \sum_{j=1}^{D} (\mu_j \phi - 1) \log y_j.$$

Since $s = -\log f$ is monotonically decreasing in f, the set $\{y : s(\mathbf{x}, \mathbf{y}) \leq c\}$ coincides with a highest-density region (HDR) conditional on \mathbf{x} . On the calibration split, compute $s_i = s(x_i, y_i)$ and define the conformal threshold as the order statistic

$$q_{1-\alpha} = \text{the } k\text{-th value of } \{s_i\}, \qquad k = [(1-\alpha)(n_{\text{cal}}+1)],$$

which guarantees marginal coverage under the split conformal scheme. For a test point x_{n+1} , set

$$t_* = -q_\alpha - \log \Gamma(\phi) + \sum_{j=1}^D \log \Gamma(\mu_j \phi), \qquad w_j = \phi(x_{n+1})\mu_j(x_{n+1}) - 1,$$

so that the exact set is

$$C_{\text{exact}}(\mathbf{x}_{n+1}) = \left\{ \mathbf{y} \in \Delta_D : \sum_{j=1}^D w_j \log y_j \ge t_* \right\}.$$

To avoid inverting this set directly, we approximate it by a containing floor triangle.

3.4. Simplex-floor HDR approximation: a convex optimization formulation

Fix \mathbf{x}_{n+1} and write $\mu = \mu(\mathbf{x}_{n+1})$, $w_j = \phi \mu_j - 1$, and $W = \sum_{j=1}^D w_j$. The exact set for the score $s(\mathbf{x}, \mathbf{y}) = -\log f(\mathbf{y} \mid \mathbf{x})$ is

$$C_{\text{exact}}(\mathbf{x}_{n+1}) = \left\{ \mathbf{y} \in \Delta_D : \sum_{j=1}^D w_j \log y_j \geq t_* \right\}, \qquad t_* = -q_\alpha - \log \Gamma(\phi) + \sum_{j=1}^D \log \Gamma(\phi \mu_j).$$

Because $\sum_j w_j \log y_j$ is concave in y when $w_j > 0$, the set above is convex. To obtain a simple set that contains $C_{\text{exact}}(x_{n+1})$, we shift the faces of the simplex by imposing lower bounds $y_i \geq \tau_i$. Each minimum floor τ_i solves the convex program

$$\min_{y \in \mathbb{R}^D} y_i \quad \text{subject to} \quad \sum_{j=1}^D y_j = 1, \quad \sum_{j=1}^D w_j \log y_j \geq t_*, \quad y_j \geq 0 \quad (j = 1, \dots, D). \tag{P}_i$$

The Lagrangian is

$$\mathcal{L}(y, \rho, \theta, \delta) = y_i + \rho \left(\sum_{j=1}^{D} y_j - 1 \right) + \theta \left(t_* - \sum_{j=1}^{D} w_j \log y_j \right) - \sum_{j=1}^{D} \delta_j y_j,$$

with $\rho \in \mathbb{R}$ (sum constraint), $\theta \ge 0$ (level constraint), and $\delta_j \ge 0$ ($y_j \ge 0$). Slater conditions holds whenever there exists $y \in \Delta_D$ with $y_j > 0$ and $\sum_j w_j \log y_j > t_*$, so Karush–Kuhn–Tucker conditions

tions (KKT) (Bertsekas, 2009) are necessary and sufficient. Under $w_j > 0$ for all j (equivalently $\lambda_j > 1$), the optimum is interior $(y_j > 0)$, yielding

$$\mathbf{1}_{\{j=i\}} + \rho = \theta \frac{w_j}{y_j} \implies y_j = \begin{cases} \frac{\theta w_j}{\rho}, & j \neq i, \\ \frac{\theta w_i}{1+\rho}, & j = i, \end{cases} \qquad \theta = \left(\frac{w_i}{1+\rho} + \frac{W - w_i}{\rho}\right)^{-1},$$

where $W = \sum_{j=1}^{D} w_j$, $\rho > 0$, $\theta > 0$. Enforcing the active level constraint $\sum_j w_j \log y_j = t_*$ leads to a one-dimensional equation for ρ ,

$$F_i(\rho) = w_i \log \rho + (W - w_i) \log(1 + \rho) - W \log(w_i \rho + (W - w_i)(1 + \rho)) + \sum_{j=1}^{D} w_j \log w_j = t_*.$$

If $w_j > 0$ for all j, then $F_i(\rho)$ is strictly increasing on $(0, \infty)$, so the root is unique. The floor for face i is

$$\tau_i = \frac{\theta w_i}{1 + \rho},$$

Given the solution ρ , we have

$$\theta = \frac{1}{\frac{w_i}{1+\rho} + \frac{W-w_i}{\rho}}, \qquad \tau_i = \frac{\theta w_i}{1+\rho}.$$

Hence, the approximate set is

$$T(x_{n+1}) = \{ y \in \Delta_D : y_i \ge \tau_i, i = 1, \dots, D \},\$$

which contains $C_{\text{exact}}(x_{n+1})$ and preserves the marginal coverage of the conformal method. To find ρ we used the function uniroot from the package stats which uses the Brent method (Brent, 2013).

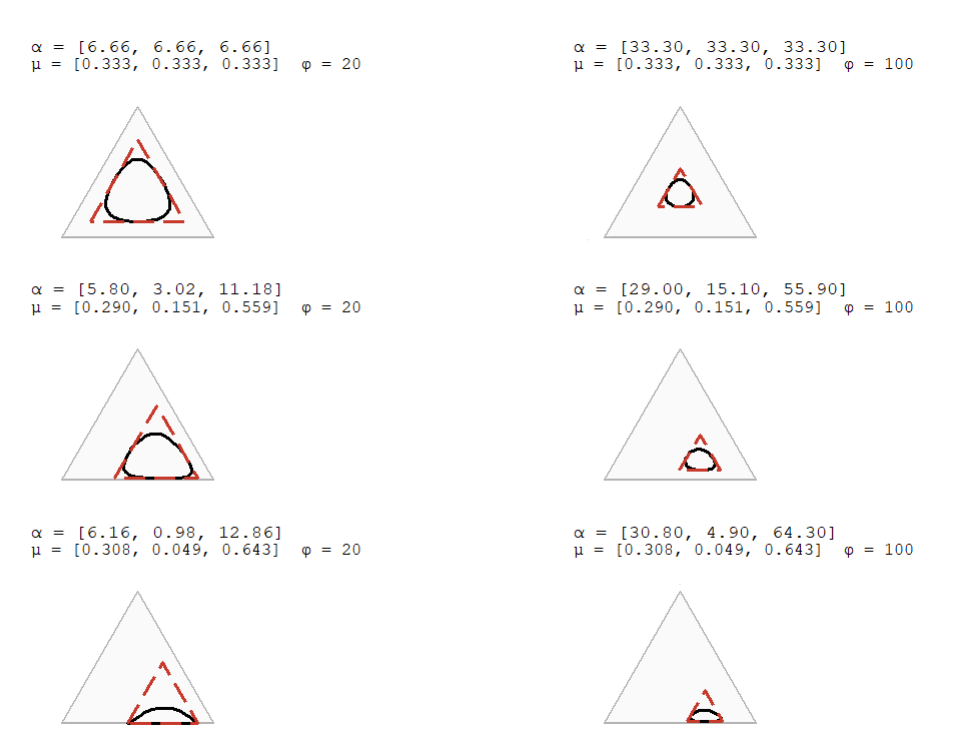


Figure 1: Plots of the HDR (black) versus the triangular approximation (red) for different parameter values.

However, the triangular HDR approximation used to obtain the prediction set leads to noticeable overcoverage, as visually evident in Figure 1. Empirical results are reported in Chapter 4 via simulations. To mitigate this overcoverage, we perform a grid search within the resulting triangle. One could in principle use a grid from the outset to construct intervals; nevertheless, because the response is multivariate and constrained to sum to one, an initial full-grid approach would be computationally prohibitive. Given the floor vector $\boldsymbol{\tau} = (\tau_1, \dots, \tau_D)$ of a polytope $T(\boldsymbol{\tau})$, construct an internal grid as follows:

- 1. Draw y_1 over $[\tau_1, 1 \sum_{j=2}^{D} \tau_j]$.
- 2. For each chosen y_1 , draw y_2 over $\left[\tau_2, 1 \tau_3 \tau_4 \cdots \tau_D y_1\right]$.
- 3. In general, after selecting y_1, \ldots, y_{k-1} (with $k \geq 2$), draw

$$y_k \in \left[\tau_k, \ 1 - \sum_{j=k+1}^D \tau_j - \sum_{j=1}^{k-1} y_j \right].$$

Let \mathcal{Y} denote the collection of grid points that lie in Δ_D . The final prediction set is

$$C(\mathbf{x}) := \left\{ \mathbf{y} \in \mathcal{Y} : \sum_{j=1}^{D} w_j \log y_j \ge t_* \right\}.$$

4. Simulation study

To assess the performance of the proposed method, we conducted a Monte Carlo simulation study with 1000 iterations. In each scenario, we generated samples of size n = 1000, splitting 70% for training, 30% for calibration, and using a fresh point for testing. For each scenario, prediction-set coverage was evaluated at a nominal level of 90%. In every scenario considered, we generated two covariates, with $x_{i22} = x_{i32} = d_{i2}$, $x_{i23} = x_{i33} = d_{i3}$, and $x_{i21} = x_{i31} = d_{i1} = 1$ for all i. All simulations were performed in R using the DirichletReg package. In Scenario 1a, the covariates were drawn from the standard uniform distribution, and the parameters were chosen so that the sample means of μ_{i1} , μ_{i2} , and μ_{i3} across the n observations are equal, while the response variance is high (ϕ near 20). In this scenario, we set $\beta_{21} = -0.3$, $\beta_{22} = 1.0$, $\beta_{23} = -0.5$, $\beta_{31} = -0.3$, $\beta_{32}=-0.5,\ \beta_{33}=1.0,\ \gamma_1=3.0,\ \mathrm{and}\ \gamma_2=\gamma_3=0.$ In Scenarios 2a and 3a, we alter selected parameters so that the component means of the response become far apart and very far apart, respectively. In Scenario 4a, we allow ϕ to depend on the covariates by setting $\gamma_2 = 0.5$ and $\gamma_3 = -0.5$. In the next scenario, the first and second covariates are generated from a Bernoulli distribution with parameter 0.5 and a Gamma distribution with parameters 3 and 6 (chosen so that the mean and variance match those of the standard uniform), respectively. Scenarios 1b-5b mirror Scenarios 1a-5a, respectively, but with $\gamma_1 = 4.6$ (so that ϕ is near 100, corresponding to a low-variance response). The scenarios used in here are the same as in Pereira & Cai (2024).

4.1. Simulation results

The results in Table 1 show that the methods Quantile Residual and HDR with grid achieve empirical coverage very close to the nominal 90% level across all scenarios, typically between 89% and 91%. By contrast, the Triangular Approximation, since we have three response components, we will refer to the HDR method as the triangular approximation, exhibits systematic overcoverage, with values between 93% and 96%, which translates into regions that are wider than necessary. In terms of efficiency, the average widths of the intervals are consistently smaller for the Quantile Residual and HDR with grid than for the Triangular Approximation.

The triangular method produces very wide boxes, whereas the conformal methods yield more compact regions. This is evident, for example, in Scenario 3b, where the widths for the Triangular

Table 1: Consolidated simulation results for the different conformal methods.

Scenario	Method	Individual Coverage (%)			Mean Width			Empirical Coverage (%)	Average Time (s)	
		y_1	y_2	y_3	y_1	y_2	y_3			
Scenario 1a	Quantile Residuals	96,6	96,6	95,0	0,4157	0,4061	0,4034	90,6	0,357	
$(\phi \approx 20)$	HDR-floor	-	-	-	0,5668	0,5668	0,5668	94,4	0,318	
	HDR-floor-grid	-	-	-	$0,\!4285$	$0,\!4194$	$0,\!4165$	90,5	0,360	
Scenario 1b	Quantile Residuals	95,2	95,9	95,5	0,1667	0,1622	0,1626	89,1	0,307	
$(\phi \approx 100)$	HDR-floor	-	-	-	0,2458	0,2458	0,2458	93,8	0,300	
	HDR-floor-grid	-	-	-	$0,\!1709$	0,1677	$0,\!1682$	89,2	0,352	
Scenario 2a	Quantile Residuals	96,2	96,1	96,1	0,3970	0,3008	$0,\!4284$	90,6	0,311	
$(\phi \approx 20)$	HDR-floor	-	-	-	0,5147	0,5147	0,5147	95,1	0,320	
	HDR-floor-grid	-	-	-	$0,\!4184$	$0,\!2921$	$0,\!4468$	90,0	0,350	
Scenario 2b	Quantile Residuals	95,4	96,3	96,3	0,1588	$0,\!1207$	0,1707	90,3	0,308	
$(\phi \approx 100)$	HDR-floor	-	-	-	0,2253	0,2253	0,2253	95,2	0,289	
	HDR-floor-grid	-	-	-	0,1646	$0,\!1236$	$0,\!1790$	90,2	0,371	
Scenario 3a $(\phi\approx 20)$	Quantile Residuals	97,2	94,5	97,5	0,2988	0,1819	0,3337	91,0	0,300	
	HDR-floor	-	-	-	0,7773	0,7773	0,7773	96,4	0,294	
	HDR-floor-grid	-	-	-	0,4933	$0,\!1374$	0,5020	90,1	0,338	
Scenario 3b	Quantile Residuals	95,7	95,5	94,8	0,1125	0,0626	0,1240	89,0	0,304	
$(\phi \approx 100)$	HDR-floor	-	-	-	0,2814	0,2814	0,2814	94,3	0,299	
	HDR-floor-grid	-	-	-	$0,\!1281$	0,0570	0,1377	89,9	0,342	
Scenario 4a	Quantile Residuals	96,8	96,8	95,9	0,3979	0,2961	$0,\!4298$	91,1	0,326	
(Hetero, ϕ_a)	HDR-floor	-	-	-	0,5456	0,5456	0,5456	95,3	0,331	
	HDR-floor-grid	-	-	-	$0,\!4376$	0,2864	0,4632	89,8	0,396	
Scenario 4b	Quantile Residuals	95,5	95,6	96,3	0,1591	0,1198	0,1713	89,5	0,309	
(Hetero, ϕ_b)	HDR-floor	-	-	-	0,2248	0,2248	0,2248	93,4	0,297	
	HDR-floor-grid	-	-	-	0,1647	$0,\!1226$	$0,\!1792$	89,5	0,352	
Scenario 5a	Quantile Residuals	95,8	96,5	95,6	0,4114	0,3963	0,3964	90,1	0,326	
$(\phi \approx 20)$	HDR-floor	-	-	-	0,5557	0,5557	0,5557	95,8	0,321	
	HDR-floor-grid	-	-	-	$0,\!4258$	$0,\!4065$	$0,\!4114$	90,5	0,380	
Scenario 5b	Quantile Residuals	96,4	96,3	95,3	0,1642	0,1587	0,1578	90,4	0,312	
$(\phi \approx 100)$	HDR-floor	-	-	-	0,2412	0,2412	0,2412	95,7	0,326	
	HDR-floor-grid	-	-	-	0,1693	0,1636	0,1649	91,7	0,340	

Approximation are more than twice those of the other methods. It is also observed that the Triangular method imposes identical widths on all components, ignoring the structure and asymmetry inherent to compositional distributions, whereas the other methods preserve cross-component differences whenever they exist. Comparing scenario pairs with higher and lower precision (labeled "a" and "b") confirms the appropriate sensitivity of the conformal methods: when precision increases, widths shrink substantially, typically by 50% to 65%, without compromising coverage, which remains on target.

In heteroskedastic settings, as in Scenarios 4a and 4b, this robustness persists: Quantile Residual and HDR with grid retain the coverage level and remain more parsimonious than the Triangular method. Relevant asymmetries across components also appear: in several scenarios, the component associated with y_2 tends to present narrower intervals than y_1 and y_3 , indicating differences in precision and average shares captured by the models. The individual coverages of the Quantile Residual method generally fall between 95% and 97%, which is consistent with simultaneous inclusion across the three coordinates, naturally pushing per-component coverage above the joint target.

Across all scenarios, except for Scenario 3a, the HDR-floor-grid and Quantile Residual methods yielded similar results. In Scenario 3a (high dispersion and the component means very far apart), the Quantile Residual method attains marginal coverages between 94.5% and 97.5%, with componentwise widths ranging approximately from 0.18 to 0.33 and empirical coverage of 91.0%. The HDR-floor-grid method achieves empirical coverage essentially at the nominal level (90.1%), however, for components y_1 and y_3 its intervals are wider than those of the Quantile Residual method, whereas for y_2 the Triangular Approximation yields a narrower interval.

It is possible to construct the conformal prediction region using a full grid over the entire simplex, without relying on the HDR approximation. However, this approach leads to a substantially higher computational burden. In contrast, the HDR approximation combined with a grid restricted to the HDR region greatly reduces computational cost. To investigate this issue, we used Scenario

1 to construct predictive intervals using both the HDR-based method and the full simplex grid. The corresponding results are reported in Table 2. We evaluated the results over 1000 and 100 Monte Carlo iterations for the response vector with three and four components, respectively. The underlying hypothesis is that by using the HDR approximation for the prediction set, fewer test points are required to achieve superior performance (e.g., in terms of coverage accuracy or width). To evaluate this, we use a grid with 100 points for the HDR-based method and 200 points for the full simplex in the three-component setting. For the four-component setting, we use 20 points for the HDR-based method and 100 points for the full simplex.

Table 2: Comparison between HDR-based grid approximation and full simplex grid.

$\overline{\phi}$	Method	Coverage (%)	Width y_1	Width y_2	Mean Width y_3	Mean Width y_4	Average Time (s)
20,09	HDR-floor-grid	90,5	0,4285	0,4194	0,4165	-	0,5244
20,09	Simplex-grid	90,5	$0,\!4321$	$0,\!4225$	0,4194	-	0,6293
134,29	HDR-floor-grid	89,2	0,1709	0,1677	0,1682	-	0,5264
134,29	Simplex-grid	89,7	0,1696	0,1679	0,1684	-	0,6277
20,09	HDR-floor-grid	89,0	0,3986	0,4054	0,4239	0,4640	0,6314
20,09	Simplex-grid	88,0	$0,\!4452$	$0,\!4337$	0,4457	0,4849	9,7665
134,29	HDR-floor-grid	89,0	0,1551	0,1628	0,1678	0,1822	0,6466
134,29	Simplex-grid	89,0	$0,\!1724$	$0,\!1739$	0,1761	0,1912	9,7192

The results in Table 2 provide clear evidence supporting the use of the HDR-based approximation. First, both methods achieve virtually identical empirical coverage across the two values of ϕ . In the three-component setting for $\phi \approx 20$, both procedures attain 90.5% coverage, and for $\phi \approx 134$, the results remain extremely close (89.2% for HDR and 89.7% for the full simplex grid). In the four-component setting, the increase in computational cost for the full simplex grid is evident: the average runtime jumps from about 0.56 seconds for the HDR-based grid to more than 9.5 seconds, while the empirical coverages remain very similar (89.0% vs 88.0% for $\phi \approx 20$ and 89.0% for both methods when $\phi \approx 134$). At the same time, the HDR-based method delivers systematically smaller marginal widths across all components, indicating a more efficient use of the probability mass. This indicates that restricting the search to the HDR region does not compromise the statistical validity of the conformal prediction intervals.

Overall, these results demonstrate that the HDR approximation provides a computationally more efficient alternative to a full simplex grid while preserving both the empirical coverage and the shape of the conformal predictive region.

5. Application

We study the determinants of household budget allocation in Italy, a classic microeconomic problem. The target is to build a predictive model for the expenditure shares assigned to three categories: food, housing, and others. Because these are parts of a whole, the response is compositional. The covariate vector \mathbf{x}_i comprises: (i) socioeconomic profile (log income and household size), (ii) market context (price indices for each category). We employ the BudgetItaly dataset with sample size n = 1729. The data are split into training (70%), calibration (20%), and test (10%) sets. To reduce the variability of the results, this splitting process was repeated 10 times and the average values are reported in Table 3. Throughout, we target a nominal coverage level of 90%.

The results from Table 3 indicate that the methods achieve the 90% nominal coverage level for all methods, with the Quantile Residuals and HDR with grid showing the smallest discrepancy 90,05% and 90,11%, respectively. In terms of efficiency, HDR with grid and Quantile Residual exhibit the lowest mean widths and are noticeably smaller than the simple HDR. The individual coverages of the Quantile Residual method are consistent with the 90,05% empirical coverage (intersection of the marginals) and reflect asymmetries between components already suggested by the widths

Table 3: Consolidated results for the application.

	Indiv	idual Co	overage (%)	Empirical Coverage (%)	\mathbf{M}	Mean Width		
Method	y_1	y_2	y_3		y_1	y_2	y_3	
Quantile Residual	93,87	98,79	92,65	90,05	0,2142	0,1999	0,2094	
HDR-floor	_	_	_	$93,\!75$	0,3072	0,3072	0,3072	
HDR-floor-grid	_	_	_	90,11	0,2204	0,2076	0,2174	

(systematically narrower intervals for y_2). In summary, for the BudgetItaly application, the Quantile Residual offers the best compromise between calibration and parsimony (coverage closest to 90% with smaller regions), closely followed by the HDR with grid. The triangular HDR serves as a fast approximation, but remains excessively conservative and less informative about the geometry of the predictive region. The visualization for four points of the test set can be visualized in the Figures 2, 3 and 4 of Appendix A.

6. Discussion

This paper develops conformal prediction procedures tailored to compositional responses that live on the simplex. We contribute two complementary constructions layered on top of Dirichlet regression: (i) a split-conformal method based on quantile residuals of the marginal Beta components (Quantile Residuals), and (ii) a density-based approach that targets highest-density regions (HDR) via a simple coordinate-floor (HDR-floor) envelope, optionally sharpened by an internal grid refinement (HDR-floor-grid).

Across extensive simulations spanning homoscedastic and heteroscedastic designs and both high-and low-precision regimes, Quantile Residuals and HDR-floor-grid achieve empirical joint coverage close to the nominal level and do so with substantially narrower regions than the unrefined HDR-floor, which is intentionally conservative. These findings are mirrored in the real-data application to household budget shares BudgetItaly, where HDR-floor-grid attains coverage closest to target with the smallest average widths, closely followed by Quantile Residuals; HDR-floor remains a useful fast baseline but yields wider, less informative sets. Together, the results indicate that calibrated and efficient uncertainty quantification on the simplex is feasible with methods that are simple to implement using standard Dirichlet regression software.

From a practical standpoint, we recommend the following: when fast computation is paramount or as a first pass, use HDR-floor to obtain a conservative envelope. When sharper sets are needed, switch to HDR-floor-grid, which recovers much of the efficiency while preserving calibration. When per-component interpretability and ease of implementation are priorities, Quantile Residuals provide a strong, robust default.

The work has limitations that suggest clear avenues for extension. HDR-floor can overcover when used without refinement, motivating adaptive grid strategies or alternative convex outer approximations that reduce slack while keeping computation manageable. Furthermore, zero inflated compositional data (Tang & Chen, 2019), common in compositional applications, call for conformal methods built on zero-inflated Dirichlet type models. In summary, the proposed conformal tools provide a practical recipe for calibrated prediction on the simplex: they are simple, geometry-aware, and empirically efficient. We hope these methods facilitate broader adoption of rigorous uncertainty quantification in compositional prediction tasks across the applied sciences.

References

- Aitchison, J. (1982). The statistical analysis of compositional data. *Journal of the Royal Statistical Society: Series B (Methodological)*, 44(2), 139–160.
- Alenazi, A. (2023). A review of compositional data analysis and recent advances. Communications in Statistics-Theory and Methods, 52(16), 5535–5567.
- Angelopoulos, A. N. & Bates, S. (2021). A gentle introduction to conformal prediction and distribution-free uncertainty quantification. arXiv preprint arXiv:2107.07511.
- Barber, R. F., Candes, E. J., Ramdas, A. & Tibshirani, R. J. (2021). Predictive inference with the jackknife+. *The Annals of Statistics*, **49**(1), 486–507.
- Barber, R. F., Candes, E. J., Ramdas, A. & Tibshirani, R. J. (2023). Conformal prediction beyond exchangeability. *The Annals of Statistics*, **51**(2), 816–845.
- Barndorff-Nielsen, O. E. & Jørgensen, B. (1991). Some parametric models on the simplex. *Journal of Multivariate Analysis*, **39**(1), 106–116.
- Bertsekas, D. (2009). Convex optimization theory, volume 1. Athena Scientific.
- Boström, H. & Johansson, U. (2020). Mondrian conformal regressors. In *Conformal and probabilistic prediction and applications*, pages 114–133. PMLR.
- Brent, R. P. (2013). Algorithms for minimization without derivatives. Courier Corporation.
- Cabezas, L. M., Otto, M. P., Izbicki, R. & Stern, R. B. (2025). Regression trees for fast and adaptive prediction intervals. *Information Sciences*, **686**, 121369.
- Chernozhukov, V., Wüthrich, K. & Zhu, Y. (2021). Distributional conformal prediction. *Proceedings of the National Academy of Sciences*, **118**(48), e2107794118.
- Cribari-Neto, F. & Lima, F. P. (2021). Resampling-based prediction intervals in beta regressions under correct and incorrect model specification. *Communications in Statistics-Simulation and Computation*, **50**(5), 1398–1416.
- Dewolf, N., De Baets, B. & Waegeman, W. (2025). Conditional validity of heteroskedastic conformal regression. *Information and Inference: A Journal of the IMA*, **14**(2), iaaf013.
- Dunn, P. K. & Smyth, G. K. (1996). Randomized quantile residuals. *Journal of Computational and Graphical Statistics*, **5**(3), 236–244.
- Espinheira, P. L., Ferrari, S. L. & Cribari-Neto, F. (2014). Bootstrap prediction intervals in beta regressions. *Computational Statistics*, **29**, 1263–1277.
- Ferrari, S. & Cribari-Neto, F. (2004). Beta regression for modelling rates and proportions. *Journal of Applied Statistics*, **31**(7), 799–815.
- Ghorbani, H. (2019). Mahalanobis distance and its application for detecting multivariate outliers. Facta Universitatis, Series: Mathematics and Informatics, pages 583–595.
- Greenacre, M. (2021). Compositional data analysis. Annual Review of Statistics and its Application, 8(1), 271–299.
- Hijazi, R. H. & Jernigan, R. W. (2009). Modelling compositional data using dirichlet regression models. *Journal of Applied Probability & Statistics*, **4**(1), 77–91.

- Hosmer Jr, D. W., Lemeshow, S. & Sturdivant, R. X. (2013). Applied logistic regression. John Wiley & Sons.
- Izbicki, R. (2025). Machine Learning Beyond Point Predictions: Uncertainty Quantification. First edition. ISBN 978-65-01-20272-3.
- Kato, Y., Tax, D. M. & Loog, M. (2023). A review of nonconformity measures for conformal prediction in regression. In *Conformal and probabilistic prediction with applications*, pages 369–383. PMLR.
- Lei, J., G'Sell, M., Rinaldo, A., Tibshirani, R. J. & Wasserman, L. (2018). Distribution-free predictive inference for regression. *Journal of the American Statistical Association*, 113(523), 1094–1111.
- Lin, J. (2016). On the dirichlet distribution. Department of Mathematics and Statistics, Queens University, 40.
- Maier, M. J. (2014). Dirichletreg: Dirichlet regression for compositional data in r. Technical Report 125, Department of Statistics and Mathematics.
- Papadopoulos, H., Gammerman, A. & Vovk, V. (2008). Normalized nonconformity measures for regression conformal prediction. In *Proceedings of the IASTED International Conference on Artificial Intelligence and Applications (AIA 2008)*, pages 64–69.
- Pereira, G. H. & Cai, J. (2024). A class of bootstrap based residuals for compositional data. arXiv preprint arXiv:2403.13544.
- Romano, Y., Patterson, E. & Candes, E. (2019). Conformalized quantile regression. Advances in Neural Information Processing Systems, 32.
- Shafer, G. & Vovk, V. (2008). A tutorial on conformal prediction. *Journal of Machine Learning Research*, **9**(3).
- Tang, Z.-Z. & Chen, G. (2019). Zero-inflated generalized dirichlet multinomial regression model for microbiome compositional data analysis. *Biostatistics*, **20**(4), 698–713.
- Tibshirani, R. J., Foygel Barber, R., Candes, E. & Ramdas, A. (2019). Conformal prediction under covariate shift. *Advances in Neural Information Processing Systems*, **32**.
- Vovk, V. (2012). Conditional validity of inductive conformal predictors. In Asian Conference on Machine Learning, pages 475–490. PMLR.
- Vovk, V., Gammerman, A. & Shafer, G. (2005). Algorithmic learning in a random world, volume 29. Springer.
- Wu, Z., Leisen, F. & Rubio, F. J. (2025). Conformalized regression for continuous bounded outcomes. arXiv preprint arXiv:2507.14023.
- Zhang, Z., Graffelman, J. & Dorn, M. (2025). A compositional approach to the analysis of white blood cell counts for early covid-19 detection. *medRxiv*, pages 2025–05.

Appendix A. Test points plots

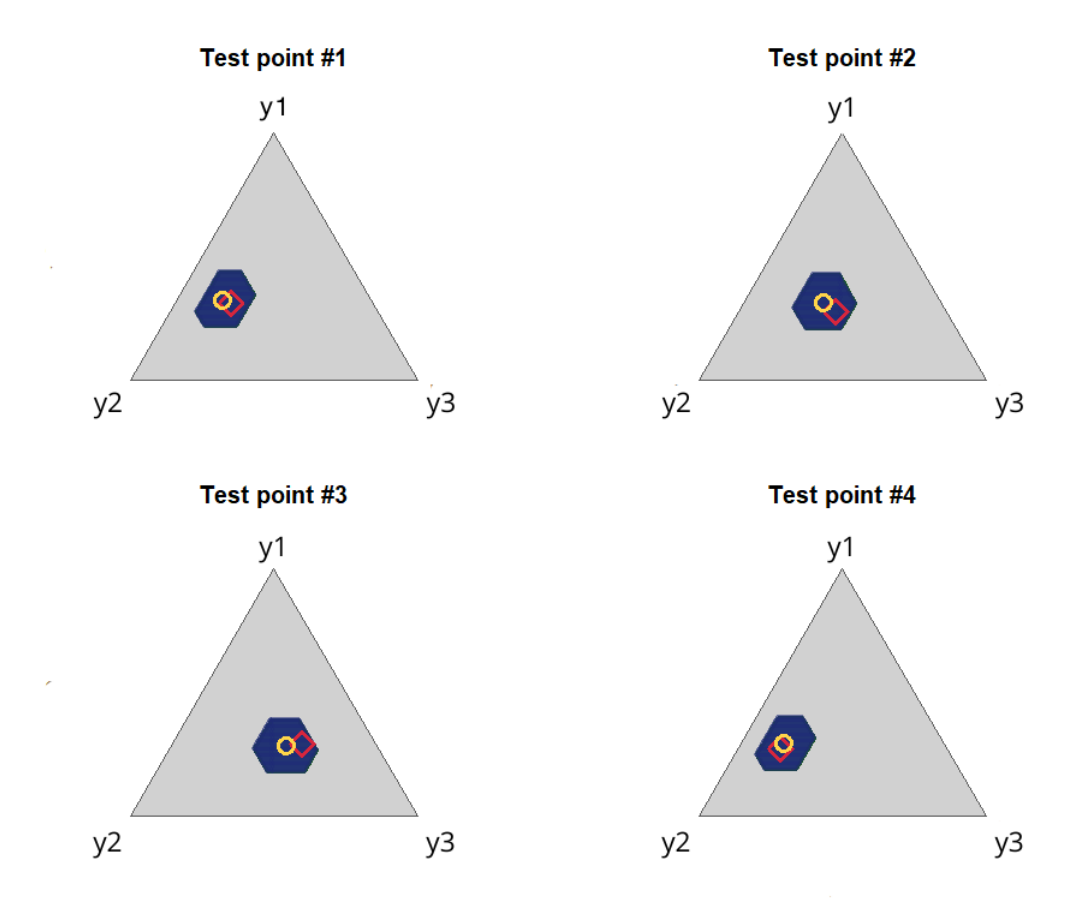


Figure 2: Test point plots for the quantile residual method. The yellow circle denotes the estimated mean, and the red diamond denotes the true test point.

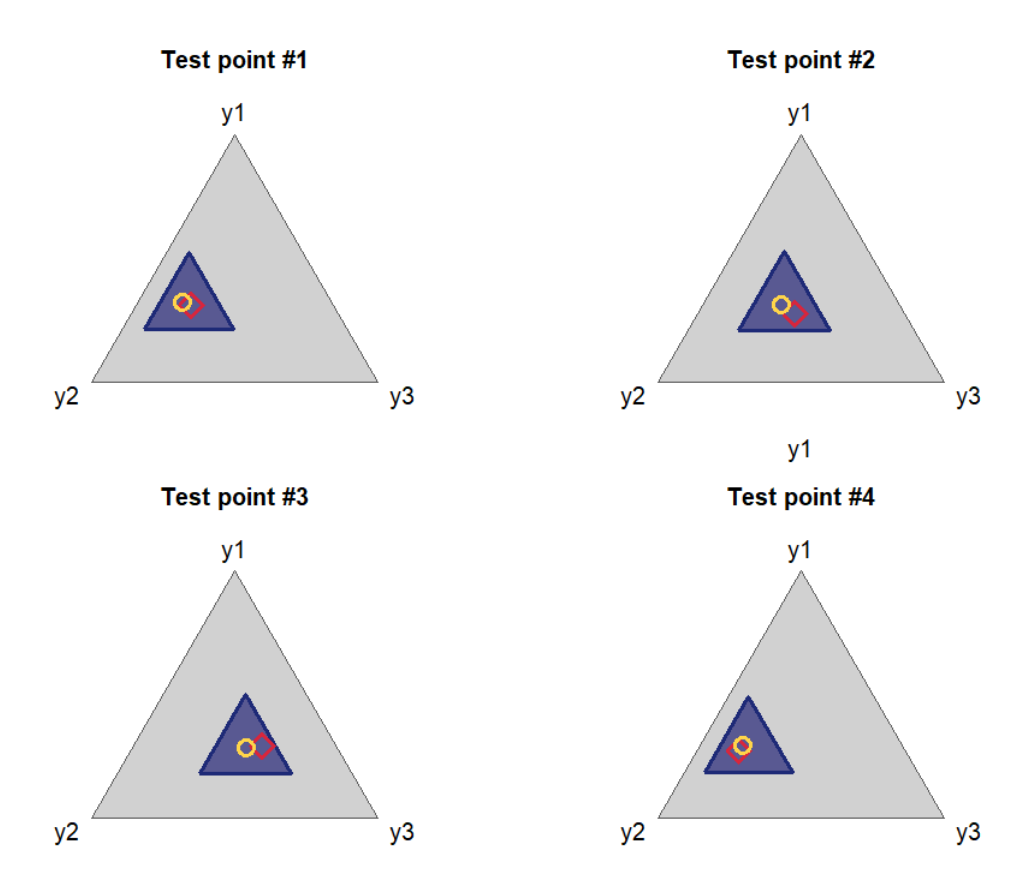


Figure 3: Test point plots for the HDR method. The yellow circle denotes the estimated mean, and the red diamond denotes the true test point.

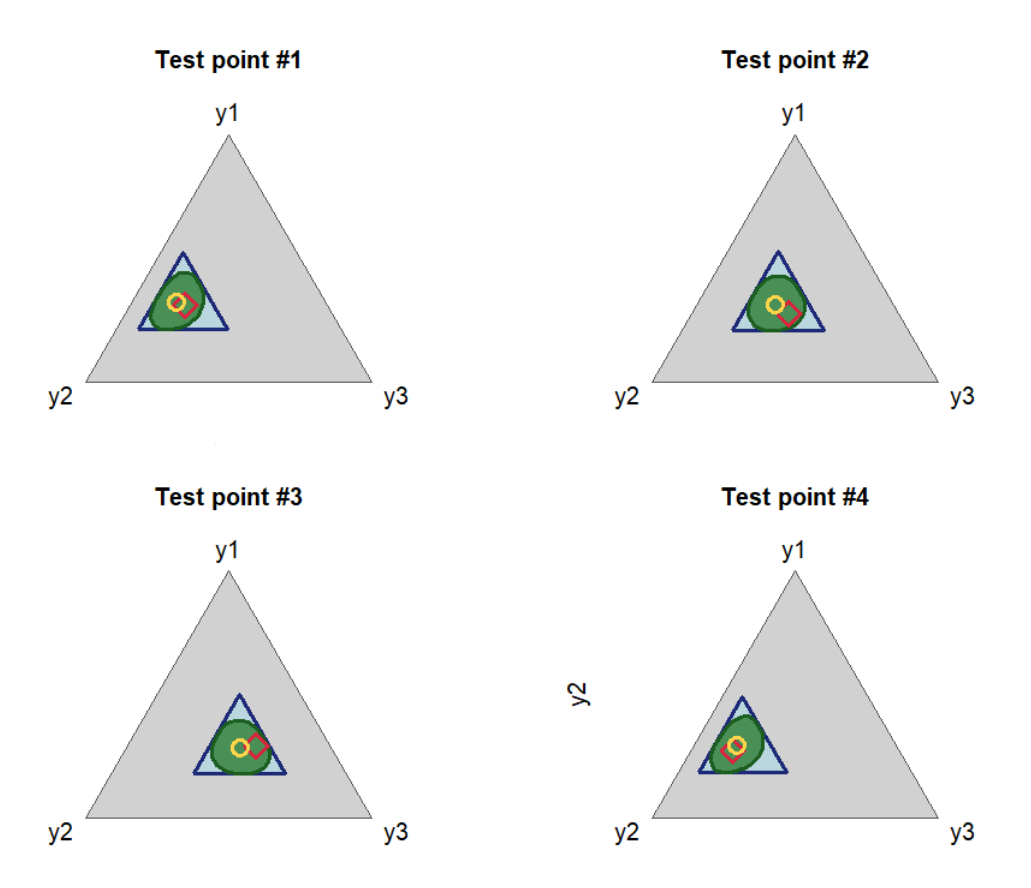


Figure 4: Test point plots for the HDR with grid method. The yellow circle denotes the estimated mean, and the red diamond denotes the true test point.

Appendix B. Split Conformal algorithm for the methods

Input: Dataset $\mathcal{D} = \{(x_i, y_i)\}_{i=1}^n$ with $y_i \in \Delta_D$; index split into training I_1 and calibration I_2 (with $n_2 = |I_2|$); model specification in (2); significance level $\alpha \in (0, 1)$.

Output: Conformal prediction set $C_{\text{split}}(x_{n+1})$ for a new covariate x_{n+1} .

- **1. Split:** Partition the data into training I_1 and calibration I_2 .
- **2. Fit:** Using I_1 , fit the Dirichlet regression in (2) and obtain parameters $\widehat{\mu}_i = \widehat{\mu}(x_i)$ and $\widehat{\phi}_i = \widehat{\phi}(x_i)$.
- **3. Calibration scores:** For each $i \in I_2$:
 - (a) For each component j = 1, ..., D, compute

$$U_{ij} = F_{\text{Beta}_j}(y_{ij}; \widehat{\mu}_{ij}, \widehat{\phi}_{ij}),$$

where F_{Beta_j} is the marginal Beta CDF induced by the fitted Dirichlet at x_i for component j.

- (b) Transform via the standard normal: $Z_{ij} = \Phi^{-1}(U_{ij})$.
- (c) Define the nonconformity score: $S_i = \max_j |Z_{ij}|$.
- **4. Conformal quantile:** Let $S_{(1)} \leq \cdots \leq S_{(n_2)}$ be the ordered $\{S_i : i \in I_2\}$. Set

$$q_{1-\alpha} = S_{(\lceil (n_2+1)(1-\alpha)\rceil)}.$$

- 5. Prediction for x_{n+1} :
 - (a) Compute $p_{\inf} = \Phi(-q_{\alpha})$ and $p_{\sup} = \Phi(q_{\alpha})$.
 - (b) Obtain $\widehat{\mu}_{n+1} = \widehat{\mu}(x_{n+1})$ and $\widehat{\phi}_{n+1} = \widehat{\phi}(x_{n+1})$. For each component j, construct the marginal interval

$$I_j(x_{n+1}) = \left[F_{\text{Beta}_j}^{-1}(p_{\text{inf}}) , F_{\text{Beta}_j}^{-1}(p_{\text{sup}}) \right].$$

(c) Return the Cartesian prediction set restricted to the simplex:

$$C_{\text{split}}(x_{n+1}) = \{ y \in \Delta_D : y_j \in I_j(x_{n+1}) \ \forall j = 1, \dots, D \}.$$

Algorithm 1: Split Conformal Prediction Set for Dirichlet Regression

- **Input:** Dataset $\mathcal{D} = \{(x_i, y_i)\}_{i=1}^n$ with $y_i \in \Delta_D$; index split into training I_1 and calibration I_2 (with $n_2 = |I_2|$); Dirichlet model specification $\lambda_j(x) = \phi(x)\mu_j(x)$; level $\alpha \in (0, 1)$.
- **Output:** Conformal prediction set $T(x_{n+1})$ (approximating HDR) for a new covariate x_{n+1} .
- **1. Split:** Partition the data into training I_1 and calibration I_2 .
- 2. Model fitting: Using I_1 , fit the Dirichlet regression and obtain the predictors

$$\widehat{\mu}(x), \qquad \widehat{\phi}(x), \qquad \widehat{\lambda}(x) = \widehat{\phi}(x)\,\widehat{\mu}(x).$$

3. Calibration scores (likelihood-based): For each $i \in I_2$, define

$$s_i = -\log f(y_i \mid x_i; \widehat{\lambda}(x_i)) = -\log \Gamma(\widehat{\phi}_i) + \sum_{i=1}^{D} \log \Gamma(\widehat{\mu}_{ij}\widehat{\phi}_i) - \sum_{i=1}^{D} (\widehat{\mu}_{ij}\widehat{\phi}_i) \log y_{ij}.$$

4. Conformal quantile: Let $s_{(1)} \leq \cdots \leq s_{(n_2)}$ be the ordered $\{s_i : i \in I_2\}$. Set

$$q_{1-\alpha} = s_{(\lceil (n_2+1)(1-\alpha) \rceil)}$$

5. Test-point parameters at x_{n+1} : Compute

$$\widehat{\mu}_* = \widehat{\mu}(x_{n+1}), \quad \widehat{\phi}_* = \widehat{\phi}(x_{n+1}), \quad \widehat{\lambda}_* = \widehat{\phi}_* \, \widehat{\mu}_*,$$

$$t_* = -q_\alpha - \log \Gamma(\widehat{\phi}_*) + \sum_{i=1}^D \log \Gamma(\widehat{\mu}_{*i}\widehat{\phi}_*), \qquad w_j = \widehat{\lambda}_{*j} - 1 = \widehat{\phi}_*\widehat{\mu}_{*j} - 1.$$

6. Coordinate floors via 1D optimization (one i at a time): For each $i \in \{1, ..., D\}$, solve the convex problem

$$\min_{y \in \mathbb{R}^D} y_i$$
 subject to $\sum_j y_j = 1$, $\sum_j w_j \log y_j \ge t_*$, $y_j \ge 0$,

obtaining τ_i . Proceed in two steps:

(a) Closed form (interior case): If $w_j > 0$ for all j (equivalently $\widehat{\lambda}_{*j} > 1$), use KKT to obtain

$$\theta = \frac{1}{\frac{w_i}{1+\rho} + \frac{W-w_i}{\rho}}, \qquad \tau_i = \frac{\theta w_i}{1+\rho}, \qquad W = \sum_{i=1}^D w_i,$$

where $\rho > 0$ is the unique root of the one-dimensional equation

$$F_i(\rho) = w_i \log \rho + (W - w_i) \log(1 + \rho) - W \log(w_i \rho + (W - w_i)(1 + \rho)) + \sum_{j=1}^{D} w_j \log w_j - t_* = 0.$$

- (b) Fallback (boundary/negative case): If some $w_j \leq 0$ (or the search fails), set $\tau_i = 0$.
- 7. Simplex-floor set: Define the floor Simplex

$$T(x_{n+1}) = \left\{ y \in \Delta_D : y_i \ge \tau_i, \quad i = 1, \dots, D \right\}.$$

8. Output: Return $T(x_{n+1})$ as the prediction set for y_{n+1} .

Algorithm 2: Split Conformal Prediction with Simplex-floor HDR Approximation